



e-ISSN: 2278-8875

p-ISSN: 2320-3765

International Journal of Advanced Research

in Electrical, Electronics and Instrumentation Engineering

Volume 10, Issue 4, April 2021

ISSN INTERNATIONAL
STANDARD
SERIAL
NUMBER
INDIA

Impact Factor: 7.122

9940 572 462

6381 907 438

ijareeie@gmail.com

www.ijareeie.com



Impact of the Fault Location, Wind Power Penetration Level and Location on Transient Stability of Power System Integrated with Doubly Fed Induction Generator

Andrew Tinkasimire¹, Keren Kaberere², James Kinyua³

Department of Electrical Engineering, Pan Africa University Institute of Basic Sciences, Technology and Innovation, Kenya^{1,2}

Project Manager, Rural Electrification and Renewable Energy Corporation, Kenya³

ABSTRACT: Renewable energy sources have undergone rapid advancement in technology and application, in order to meet the ever growing global demand for energy. Their integration into the grid has caused challenges to the reliability and stability of power systems. Specifically, the wind power generation has accounted for the large share of renewable energy, and its integration has affected the system inertia, thus impacting power system stability. Therefore, analyzing the impact of the wind power generation on the system stability is significant to improve the system security. In this paper, a Doubly Fed Induction Generator was applied to study the effect of wind power on the power system transient stability. Although the impact of wind power integration on the system stability has been studied in detail, the impact of fault location on the system's transient stability is not reported in literature. In this paper, the impact of fault location with different levels of wind power integration on the system transient stability was investigated. The IEEE 9 Bus system was studied using DIgSILENT PowerFactory. The time domain results showed that the wind power integration increases or decreases the system transient stability, depending on the location of the fault and the wind power penetration level.

KEYWORDS: Wind Power penetration, Transient Stability, Fault Location, Rotor Angle.

I.INTRODUCTION

In recent years, there has been an increase in the world population, which has increased the global energy usage. Conventional sources of energy have been used in the past to meet this growing demand. However, this has caused negative effects on the environment and energy policies have shifted towards renewable energy. Renewable energy sources are favoured because they are inexhaustible in nature. Therefore, there are ongoing efforts to integrate them into the main grid.

Wind energy is an infinite energy source with limited impacts on the environment. It has proven to be one of the most effective renewable energy sources, with relatively high efficiency, costs of power generation are competitive with conventional sources and a means to reduce carbon emissions [1]. The majority of the wind turbines are equipped with Doubly Fed Induction Generators (DFIGs). With the Wind Power System, the DFIG is grid connected at the stator terminals and the rotor terminals are connected via the variable frequency AC-DC-AC converter. The converter consists of the Grid Side converter (GSC) and the Rotor Side Converter (RSC), which are linked via a back-to-back dc link capacitor [2]. The DFIG offers a number of benefits as compared to other wind turbines such as decoupled controllability, improved power quality, affordable and high power conversion efficiency [3].

If there is high penetration of wind power generation in an interconnected grid, it lowers the inertia of the power system. Thus, the integration of wind power impacts the system rotor angle stability, which has been an area of concern [4]. Therefore, it is important to analyze the impact of location of wind power integration on the system transient stability.



The power network is affected by both the small and large disturbances. Most importantly, the network should be able to withstand large disturbances such as loss of a generator or transmission line [5]. If the system is able to withstand a large fault, the system transient stability is recovered. Stability could be recovered after one of the power components has tripped, or the network is divided into islands in order for the system to remain operational. Sustained faults will lead to an increased angular separation and decrease in bus voltage. The low system voltages will lead to cascading outages and the main part of the network will shut down.

In a traditional power system, the synchronous generator is an essential part of the power system that contributes to network stability. In case of a large disturbance, the exciter regulates the voltage of the system. However, the Synchronous Generator (SG) has capability limits, so in case the large disturbance is significant, the rate of change of the rotor angle will increase, bringing the machine closer to loss of synchronism. Compared with the SG, the wind turbines are seen as weak capability for riding through faults due to induction generators and power electronics interface [6]. The voltage sag can lead to an increase in the rotor current, which can destroy the valves. For protection purposes, the DFIG converters have to be tripped from the system and then the wind generator should be disconnected from the power system [7].

The dynamic response of the DFIG depends on the control operation of the converters in the system, which is different from the operation of the synchronous generators. With the increase of wind power penetration into the grid, it has become important to effectively evaluate the impact of integration of DFIG on the transient stability. The influence of the DFIG integration on the power system has been studied considerably and the rotor angle response to the fault has been investigated. The authors in [8] investigated different network structures, penetration levels of the DFIG and points of common coupling to evaluate the impact of the DFIGs on system stability. It was deduced that the power angle characteristics are improved with increase in the wind power. The authors in [9] investigated the relationship between wind power generation and the rotor angle stability of conventional synchronous generators, with the viewpoint of controlling reactive power using the variable speed wind turbine generators in the network. The authors deduced that wind power generation system can be utilized to control voltage and reactive power in the system and boost stability. An evaluation of the wind turbine contribution to the frequency control of the non-interconnected island systems was done in [10]. The authors reported that the wind turbines provided crucial active power during transient events that boosted the system stability. A novel frequency regulation by DFIG-based wind turbines was presented in terms of coordinating inertial control, rotor speed control and pitch angle control for the low, medium, and high wind speed mode [11].

In [12], the dynamic mathematical model of the DFIG suitable for transient stability analysis was studied. It was demonstrated that the proportional gain of the speed and voltage control could be used to enhance the stability of the DFIG. The authors in [13] presented a detailed analysis of the windmill mechanical models for transient stability analysis of wind power systems. A two-shaft mass model produced better results for transient stability analysis of wind power generation systems, as compared with the single shaft mass model. The model of the wind turbine in the DFIG to demonstrate that the transient stability can be maintained after a disturbance was investigated in [14]. The authors deduced that a complete DFIG model was suitable for the analysis of the interaction between the wind system and the power system. The authors in [7] concluded that the transient stability of the 39-bus system improved with wind integration. The analysis of the impact of large-scale wind generation on the transient and voltage stability of the system was investigated in [15]. The investigation was done with different wind penetration levels. It was concluded that the Static Voltage Compensator (SVC) enhanced the wind power penetration when compared with a system with no SVC. The interactions between the wind farm and synchronous generator were analyzed in [16] with consideration of wind power penetration level and load models during simulation comparisons. The analysis showed that under specific fault conditions, the increased wind power penetration level improved the transient stability. In [17], it was deduced that the increasing wind power penetration in the system worsens the transient stability performance. A new quantitative assessment of transient stability for power systems integrated with DFIG was proposed in [18]. The results showed that power systems integrated with wind energy are more sensitive to transient events than the conventional systems. The authors in [19] evaluated the impact of the DFIG integrated in the power system on the transient stability, considering key factors such as the location of the wind farm and the wind speed. The evaluation showed that increasing wind power penetration reduced the system stability.

There has been considerable research done on the transient stability performance of power systems with wind power integration. However, the fault location, location of the DFIG and level of wind power penetration, as factors affecting the wind integrated system performance is yet to be studied. Therefore, the study of the system performance is simulated using DIGSILENT PowerFactory to determine the transient stability of a power system integrated with DFIG system.



The paper is organized as follows: Section 1 is an introduction and the system components modelling is presented in Section 2. The test system and the simulated scenarios are presented in Section 3 whereas the simulation results and conclusions are presented in sections 4 and 5, respectively.

II. POWER SYSTEM MODELLING

A. Modeling of the Wind Power Generation System

A wind power generation system consists of the prime mover, DFIG, gear box, converters and the controller. The prime mover extracts kinetic energy from the wind using the turbine blades and converts it into mechanical torque which is used by the induction generator to supply electrical power.

The stator winding is connected to the power system directly whereas the rotor is connected to the grid through back-to-back converters. The rotor side converter is connected to the slip rings of the rotor and the grid side converter is connected to the external power system. The DC capacitor connected in between the converters is the DC Voltage source for AC/DC power transformation. The structure of the DFIG wind power generation system is shown in the figure 1 [20] .

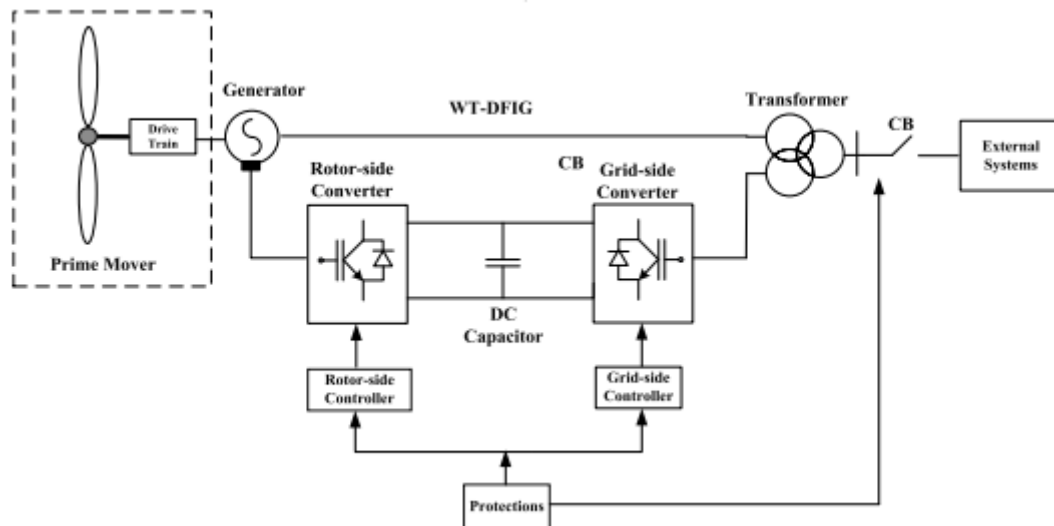


Figure 1; Wind Power System

The kinetic energy extracted from the wind by turbine blades is given by

$$P_m = \frac{1}{2} \rho \pi R^2 V_w^3 C_p \tag{1}$$

Where P_m is the mechanical power from the wind turbine, ρ is the air density, R is the blade radius of wind turbine, V_w is the wind speed, C_p is the power coefficient and a function of the tip speed ratio λ and blade pitch angle β which is given by

$$C_p(\lambda, \beta) = \frac{1}{2} \left(\frac{RC_f}{\lambda} - 0.022\beta - 2 \right) e^{-0.225 \frac{RC_f}{\lambda}} \tag{2}$$

$$\lambda = \frac{R\omega_t}{V_w} \tag{3}$$

Where C_f is the blade design constant coefficient and ω_t is the rotational speed of the wind turbine.

When the wind speed increases above the rated speed, the blade pitch angle controller is applied in the wind turbine. The blade pitch angle consists of proportional integral (PI) controller and servomechanism and it controls the speed



deviation of the rotor blades. Beyond the rated wind speed, the speed deviation is regulated by the pitch angle controller.

The drive train is represented by the generators high speed shaft and the turbine low speed shaft, coupled with a gear box. The model is given by;

$$2H_t \frac{d\omega_t}{dt} = T_m - T_{sh} \quad (4)$$

$$2H_g \frac{d\omega_t}{dt} = T_{sh} - T_{em} \quad (5)$$

$$\frac{d\theta_{tw}}{dt} = \omega_t - \omega_\tau \quad (6)$$

$$T_{sh} = K_{sh} * \theta_{tw} + D_{sh} * \frac{d\theta_{tw}}{dt} \quad (7)$$

$$T_m = \frac{P_m}{\omega_t} \quad (8)$$

$$T_{em} = \frac{P_s}{\omega_\tau} \quad (9)$$

Where H_t is the inertia constant of the wind turbine, H_g is the inertia constant of the generator, T_m is the mechanical torque of the wind turbine, T_{em} is the electromagnetic torque of the generator, T_{sh} is the shaft torque, θ_{tw} is the shaft twist angle, K_{sh} is the shaft stiffness coefficient, D_{sh} is the damping coefficient, P_s is the active power of the generator's stator winding.

B. Modelling of the DFIG converter

The dynamic model of the DFIG rotor side is expressed as

$$\frac{dE'_d}{dt} = s\omega_s E'_q - \frac{\omega_s L_m}{L_r} V_{rq} - \frac{1}{T'_0} [E'_d + (X_s - X'_s)I_{sq}] \quad (10)$$

$$\frac{dE'_q}{dt} = -s\omega_s E'_d - \frac{\omega_s L_m}{L_r} V_{rd} - \frac{1}{T'_0} [E'_q - (X_s - X'_s)I_{sd}] \quad (11)$$

Where E'_d is the d axis voltage behind the transient reactance, E'_q is the q axis voltage behind the transient reactance, V_{rd} is the d axis voltage on rotor side of DFIG, V_{rq} the q axis voltage on rotor side of DFIG, I_{sd} is the d axis current on stator side of DFIG, I_{sq} is the q axis current on stator side of DFIG, s is the rotor slip of DFIG, ω_s is the synchronous rotational speed, L_s is the self inductance on the stator side of DFIG, L_m is the mutual inductance on the stator side of DFIG, T'_0 is the circuit time constant on the rotor side of DFIG, X_s is the reactance on the stator side of DFIG, X'_s is the transient reactance on the stator side of DFIG.

The dynamic model of the grid side converter of the DFIG is expressed as

$$\frac{X'_s}{\omega_s} \frac{dI_{sd}}{dt} = V_{sd} - \left[R_s + \frac{1}{\omega_s T'_0} (X_s - X'_s) \right] I_{sd} - (1-s)E'_d + \frac{L_m}{L_r} V_{rq} + \frac{1}{\omega_s T'_0} E'_q + X'_s I_{sq} \quad (12)$$

$$\frac{X'_s}{\omega_s} \frac{dI_{sq}}{dt} = V_{sq} - \left[R_s + \frac{1}{\omega_s T'_0} (X_s - X'_s) \right] I_{sq} - (1-s)E'_q + \frac{L_m}{L_r} V_{rd} + \frac{1}{\omega_s T'_0} E'_d + X'_s I_{sd} \quad (13)$$

Where V_{sd} is the d -axis voltage on the DFIG stator, V_{sq} is the q -axis voltage on the stator side of DFIG, R_s is the resistance on the stator side of DFIG.

Neglecting the power losses in the rotor side and grid side converters, the active power can keep balanced through the two converters, given by;

$$P_{rc} = P_{gc} + P_{cap} \quad (14)$$

Where P_{rc} is the active power in the rotor side converter, P_{gc} is the active power in the grid side converter, P_{cap} is the active power in the DC capacitor. The expressions are given by;



$$P_{rc} = V_{rd}I_{rd} + V_{rq}I_{rq} \quad (15)$$

$$P_{gc} = V_{sd}I_{sd} + V_{sq}I_{sq} \quad (16)$$

$$P_{cap} = V_{dc}I_{dc} = C_{dc}V_{dc} \frac{dV_{dc}}{dt} \quad (17)$$

Where I_{rd} is the d-axis current on rotor side of DFIG, I_{rq} is the q-axis current on rotor side of DFIG, I_{gd} is the d-axis current of the grid side converter, I_{gq} is the q-axis current of grid side converter, V_{dc} is the DC voltage of DC capacitor, I_{dc} is the DC current of DC capacitor, C_{dc} is the capacitance of DC capacitor. Therefore, the dynamic model of the DC link is expressed as

$$\frac{dV_{dc}}{dt} = \frac{1}{C_{dc}V_{dc}} (V_{rd}I_{rd} + V_{rq}I_{rq} - V_{sd}I_{gd} - V_{sq}I_{gq}) \quad (18)$$

C. Swing Equation

Under normal operating conditions of the synchronous generator, the relative position of the rotor angle and the resultant axis of the magnetic field is constant. When a fault occurs, the rotor will speed up or slow down depending on the air gap magnetomotive force that rotates synchronously, resulting in relative motion. This motion is represented by the swing equation.

$$\frac{H}{\pi f_0} \frac{d^2\delta}{dt^2} = \frac{H}{180f_0} \frac{d^2\delta}{dt^2} = P_m - P_e \quad (19)$$

Where f_0 is natural frequency, H is the inertia constant, δ is the rotor angle of the generator, P_m is the input mechanical power and P_e is the electrical power developed by the generator.

When the rotor acceleration reaches the maximum power transfer, the kinetic energy gained during the acceleration period has not been entirely spent, which results into a large rotor speed and the rotor angle, δ continues to increase. After exceeding the maximum power transfer, P_e is smaller than P_m , making the rotor acceleration to proceed. The speed and angle of the rotor continuously increase, edging the machine closer to instability.

III.METHODOLOGY

Stability is analyzed based on the rotor angle. The rotor angle is measured against the bus voltages in the multi machine system. The relative rotor angles for individual machines were referenced based on the voltage angle, rotor angle and the reference machine angle [15].

The reference machine voltage angle was set to zero and the voltage phase of other buses are measured against the reference machine voltage vector.

If the rotor angle difference between the machines is greater than 90 degrees, the system edges closer to loss of stability and the voltage drop is instantaneous.

A. Test System

The modified IEEE 9 bus system was used for the study and modelled using DIgSILENT PowerFactory. The system's single line diagram is given in figure 2 [16].

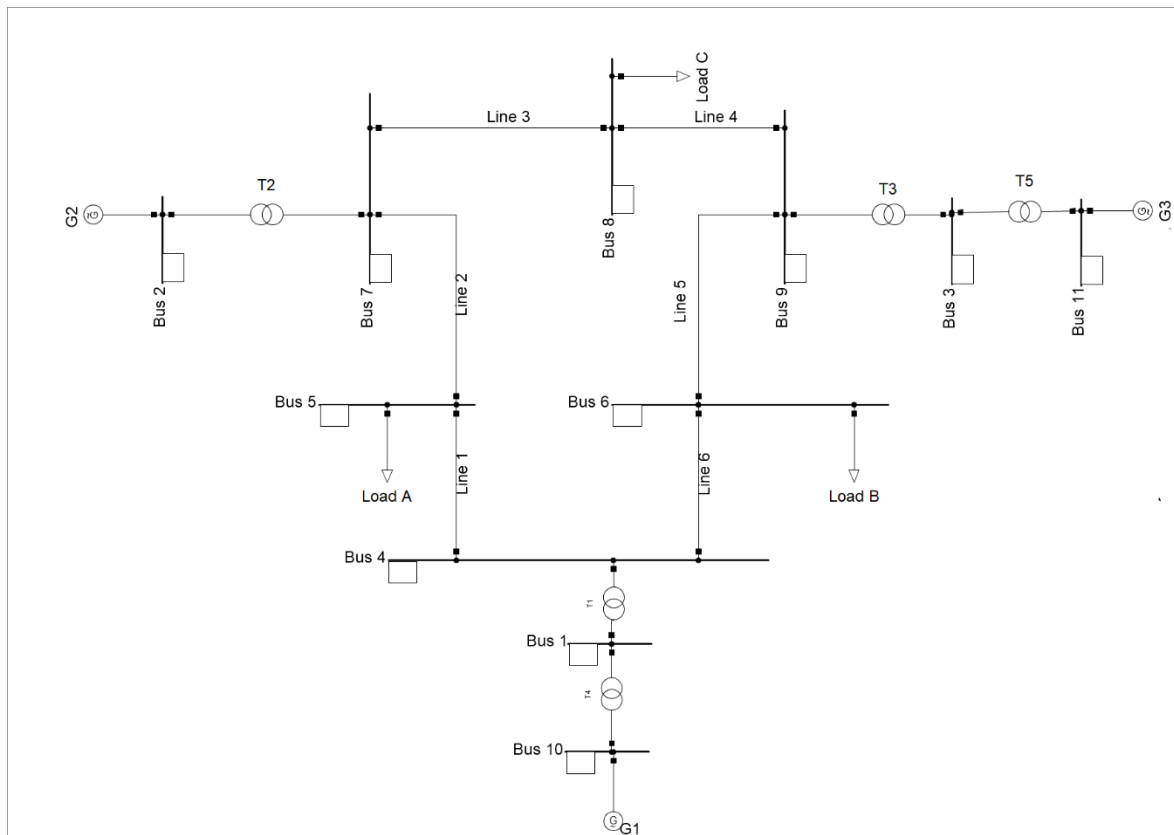


Figure 2; Modified IEEE 9 Bus system

The operating conditions are given in the appendix. The generators are manually controlled in order to evaluate the effect of the wind power system dynamics on the power system. The synchronous generators are sixth order models and the static load models were used with active and reactive power. The transmission lines are modelled as pi model and the transformer resistance losses are neglected.

B. Scenario Formulation

Simulations were run for different scenarios of fault location and wind power generation replacing either synchronous generators G2 or G3. The scenarios are as tabulated in table 1:

Table 1: Simulation scenarios

Fault location	Wind Power replacing G2 output (MW)-Scenario A			Wind Power replacing G3 output (MW)-Scenario B		
	25	50	163	25	50	85
Line 2	25	50	163	25	50	85
Line 5	25	50	163	25	50	85

Each of the DFIG units used had a capacity of 5MW. The output of the conventional generator G3 was gradually replaced by integrating 25MW, 50MW wind power before full replacement of the synchronous generator. The same procedure was followed for generator G2. The full capacity of the two generators is different because the generator G2 was operating at a capacity of 163MW and the generator G3 was operating at a capacity of 85MW.

The fault was introduced at 30% of the line 2 and line 5 at 1 second and the circuit breakers on both ends of the line were opened after 100 milliseconds. Line 2 and Line 5 were considered in this study because they are long lines and the most heavily loaded lines in the system. The system response of the two generators G2 and G3 were studied, with the



system response for G2 studied while wind integration was on G3 bus and G3 studied while the wind integration was on G2 bus. The system response to the three phase fault was analyzed in correspondence with the gradual increment of wind power penetration replacing the active power output of the synchronous generators G2 and G3.

The electromechanical simulations are carried out in DIgSilent and the Critical Clearing Time is determined using the critical fault screening program in DIgSilent [17].

IV.RESULTS AND DISCUSSIONS

A. Wind integration at G3 bus

In scenario A, the wind power was integrated at bus 11 to gradually replace the active power output of generator G3. The figure 3 represents the rotor angle response of generator G2 to the three phase fault on Line 2.

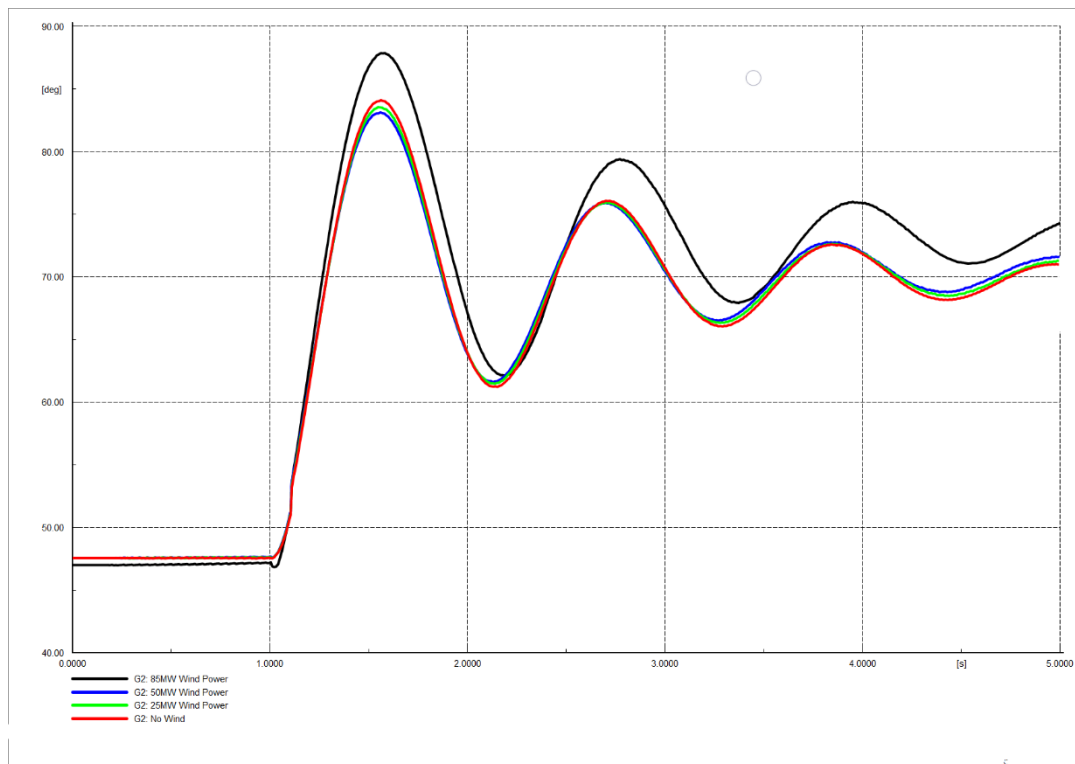


Figure 3; Rotor Angle response of G2 to a fault at Line 2

It can be observed from Figure 3 that the first swing increased with increase in wind power penetration. The increasing amplitude of the angular oscillations occurred with increase in wind power integration. This implied that the transient stability of the generator reduced as the wind power integration increased.

The figure 4 shows the rotor angle response of the generator G2 when the fault is located on Line 5.

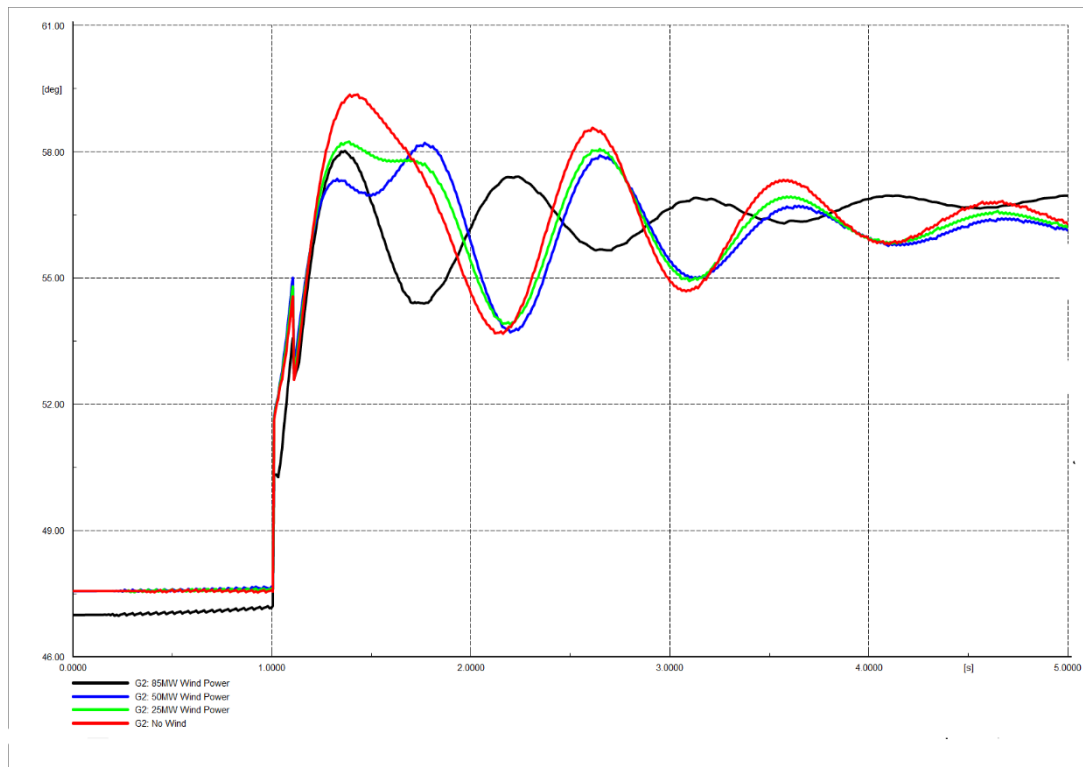


Figure 4; Rotor Angle response of G2 to a fault on Line 5

When the fault is introduced at line 5, the amplitude of the angular oscillations decreased with increasing wind penetration. The settling time of the oscillations reduced as the wind integration increased. This implied that the transient stability of the generator improved with increasing wind integration.

B. Wind integration at G2

In scenario B, the wind power was integrated on bus 2, gradually replacing the active power capacity of the synchronous generator G2. A three phase fault was applied at line 2 and the angular response of G3 was studied. From figure 5 below, the amplitude of the angular oscillations reduced with increasing wind penetration. The settling time of the oscillations reduced with increasing wind power penetration. This, implied an improvement in the transient stability of the generator G3 as the wind power penetration increased on generator G2.

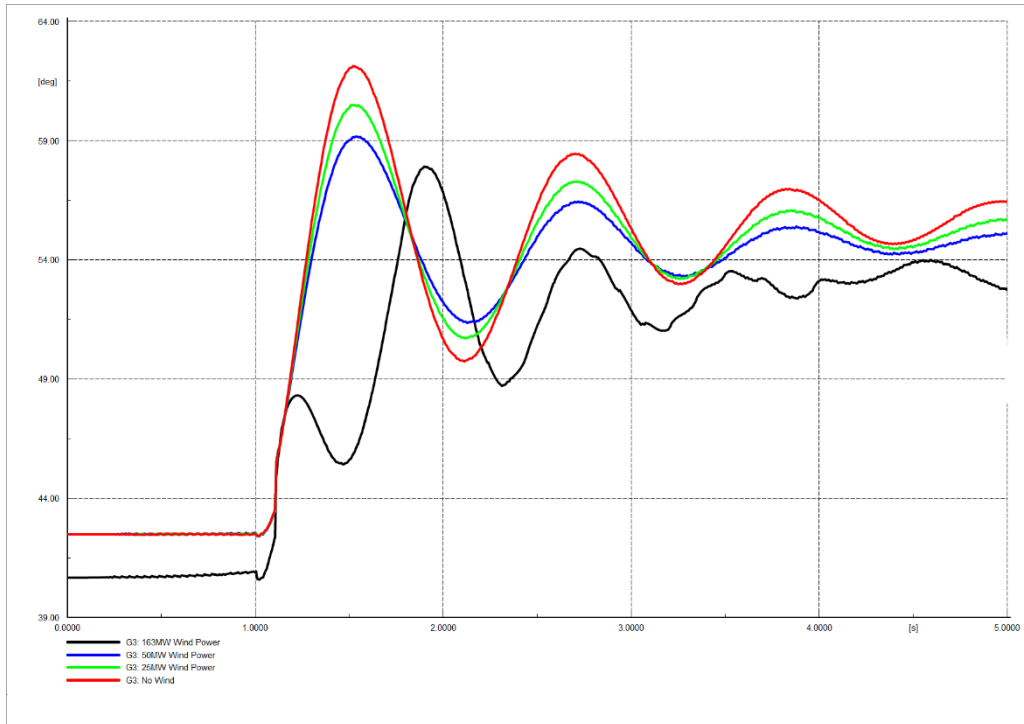


Figure 5; Rotor Angle response of G3 to a fault at Line 2

When the fault occurred on line 5 as shown in figure 6, the rise time of the angular oscillations increased with wind power penetration increase. The settling time of the oscillations increased, implying that the generator G3 took longer to attain transient stability, as the wind integration on generator G2 increased.

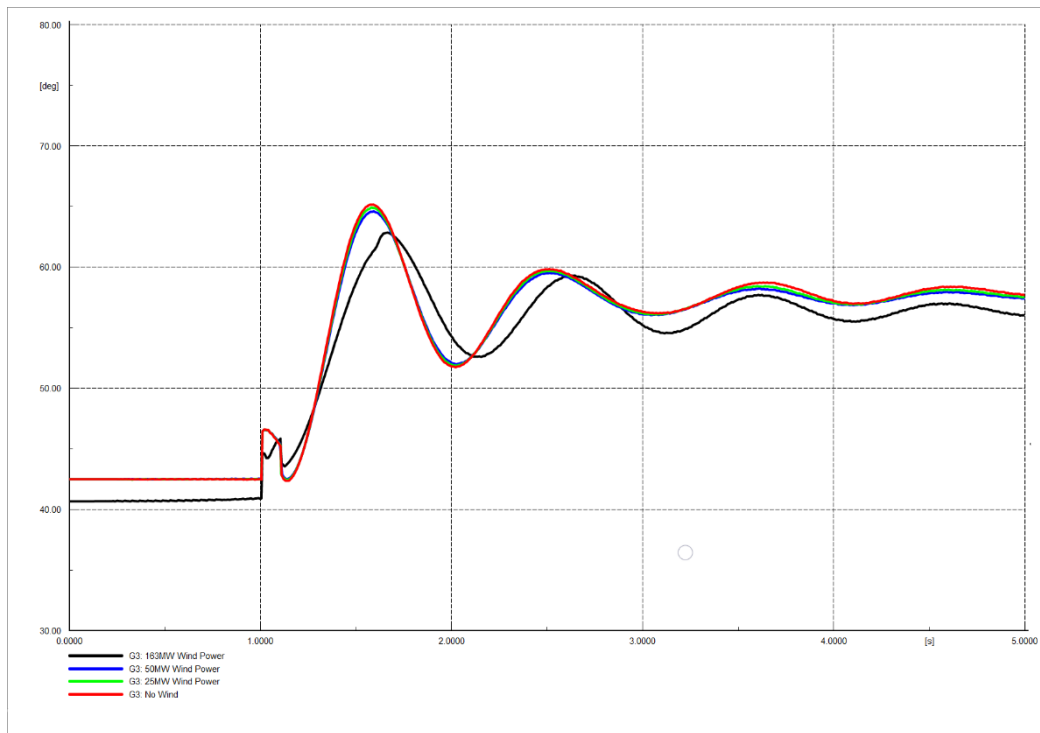


Figure 6; Rotor Angle response of G3 to fault at Line 5



C. Critical Clearing Time

The Critical Clearing Time (CCT) of the two generators was tabulated as shown in table 2 below. The table shows the results for the fault at Line 2 and Line 5.

Table 2; Critical Clearing Time of the Generators G2 and G3 for a fault at Line 2 and Line 5

Fault location	CCT of generator G3 for wind integration on G2 bus (ms)				CCT of generator G2 for wind integration on G3 bus (ms)			
	No Wind	25	50	163	No Wind	25	50	85
Wind Capacity (MW)								
Fault at Line 2	477	620	869	2606	477	439	385	241
Fault at Line 5	778	770	762	109	778	1450	1874	1889

From the above table 2, it was observed that as the wind power penetration increased, the CCT for the generator reduced when it was electrically close to the fault and increased when the fault was located farther from the generator.

From the results above, the stability in the wind power integrated systems depends on the following;

Fault location

1. When the fault occurred close to the wind farm, the transient stability of the generator increased with wind power integration.
2. When the fault occurred farther from the wind farm, the transient stability of the generator reduced with increasing wind power integration.

Location of the wind farm

The location of the wind farm in the power system improved or reduced the transient stability, depending on the locations of the fault in the system.

Wind penetration

Increasing wind power penetration into the power system improved or worsened the angular stability, depending on the location of the fault.

V. CONCLUSION

The rotor angle stability of the wind power integrated systems was studied and the system response of the rotor angle for the synchronous generators G2 and G3 were obtained. The impact of location of the wind farm, wind penetration level, and fault location on the transient stability performance of the power system were investigated. The results showed that the system stability of the wind integrated power system was affected by the wind penetration levels, location of the wind farm and the location of the fault.

The simulation results of the modified IEEE 9 Bus system showed that the wind penetration increases or decreases the transient stability of the system depending on the fault location and the wind power penetration level. It was shown that DFIG integration improved the system transient stability if the fault was located close to the wind farm. On the other hand, the transient stability deteriorated if the fault occurred farther from the wind farm.



APPENDIX

Modified IEEE 9-bus system data

The network values in per unit form are to the common base of 250MVA and 230kV to the high voltage of the transformer

Generator Data

Type	G1	G2	G3
Nominal Power (MVA)	512	270	125
Nominal Voltage (L-L)	24	18	15.5
X_d (pu)	1.7	1.7	1.22
X'_d (pu)	0.27	0.256	0.174
X''_d (pu)	0.2	0.185	0.134
T'_{do} (s)	3.8	4.8	8.97
T''_{do} (s)	0.01	0.01	0.033
X_q (pu)	1.65	1.62	1.16
X'_q (pu)	0.47	0.245	0.25
X''_q (pu)	0.2	0.185	0.134
T'_{q0} (s)	0.48	0.5	0.5
T''_{q0} (s)	0.0007	0.0007	0.07
R_a (pu)	0.004	0.0016	0.004
X_L (pu)	0.16	0.155	0.0078
H (s)	2.6312	4.1296	4.768

Load Data

Item	Load	Active Power (MW)	Reactive power (MVar)
1	A	125	50
2	B	90	30
3	C	100	35

System Operating Conditions

Item	Parameter	G1 (Slack Bus)	G2 bus	G3 bus
1	Voltage (pu)	1.04	1.025	1.025
2	Power angle (°)	0	9.3	4.7

Transmission line data (The lines are assumed to be 1km long)

Item	Line Section	Resistance (Ω /km)	Reactance (Ω /km)	Susceptance (μ /km)
1	4-5	5.29	44.965	332.7
2	4-6	8.993	48.668	298.69
3	5-7	16.928	85.169	578.45
4	7-8	4.4965	38.088	281.66
5	8-9	6.2951	53.3232	395.08
6	6-9	20.631	89.93	676.75

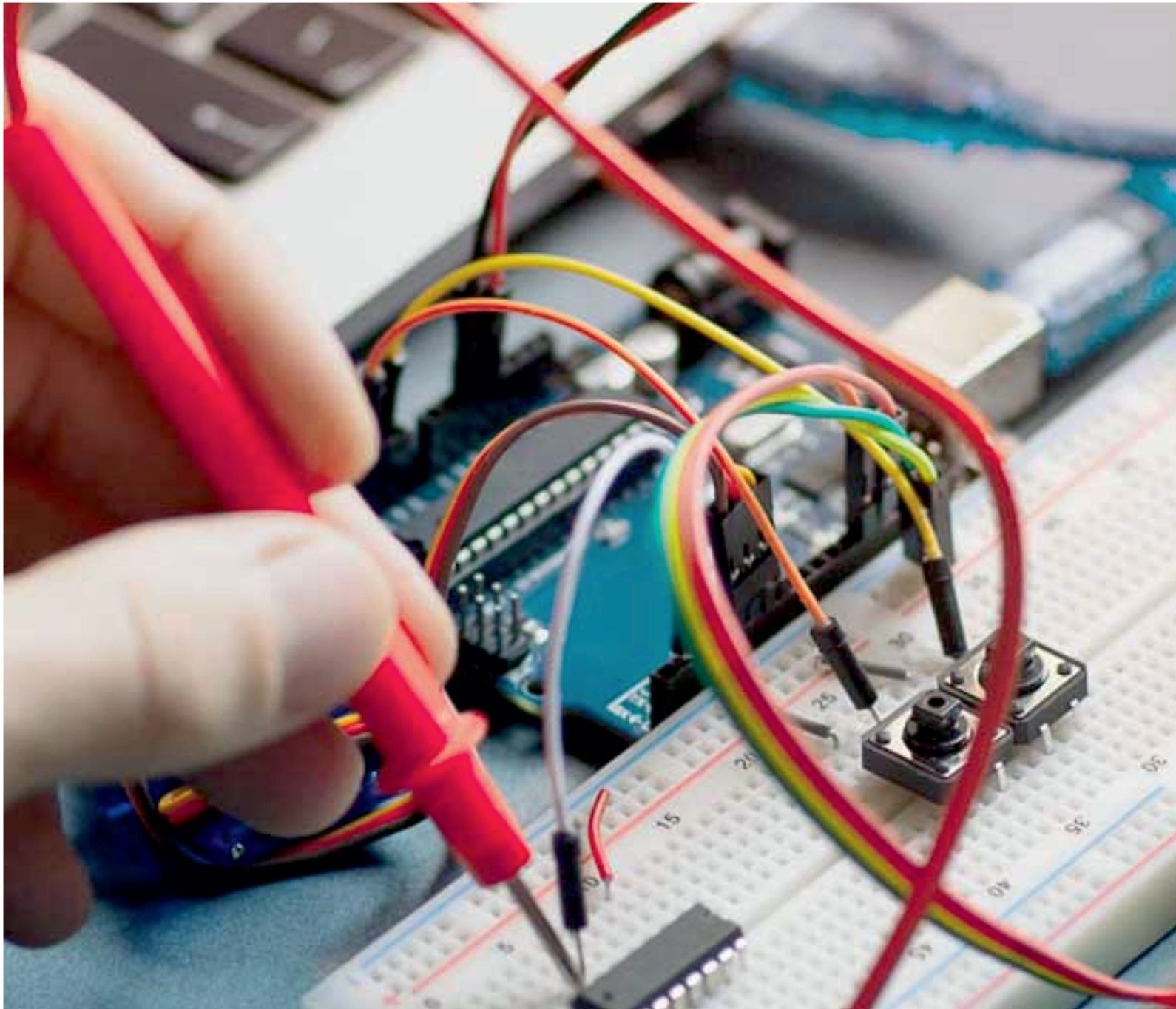
Transformer data

Item	Parameter	T_1	T_2	T_3
1	Rated MVA	250	200	150
2	Rated kV	16.5/230	18/230	13.8/230
3	Positive sequence reactance (pu)	0.144	0.125	0.0879
4	Positive sequence resistance (pu)	0	0	0



REFERENCES

- [1] Castro Sayas F., Allan R.N., " Generation Availability of Wind Farms," in *IEE Proceedings on Gen., Trans., and Distr.*, 1996.
- [2] R. Pena, J. C. Clare, and G. M. Asher, "Doubly fed induction generator using back-to-back PWM converters and its application to variable-speed wind-energy generation," *IEE Proc. – Electric Power Applications*, vol. 143, no. 3, pp. 231-241, 1996.
- [3] Fernández, L.M., Jurado, F., Saenz, J.R, "Aggregated dynamic model for wind farms with doubly fed induction generator wind turbines," *Renew. Energy*, vol. 33, pp. 129-140, 2008.
- [4] Liu, S.; Li, G.; Zhou, M., "Power system transient stability analysis with integration of DFIGs based on center of inertia," *CSEE J. Power Energy System*, vol. 2, pp. 20-29, 2016.
- [5] P. Kundur, *Power System Stability and Control*, New York: McGraw-Hill, 1994.
- [6] Wei Qiao, Ronald G. Harley, "Effect of Grid-Connected DFIG Wind Turbines on Power System Transient Stability," *IEEE Power and Energy Society General Meeting*, 2008.
- [7] Wei Qiao, and Ronald G. Harley, , "Effect of Grid-Connected DFIG Wind Turbines on Power System Transient Stability," *IEEE Power Transactions*, 2008.
- [8] Bei Wang. Lin Zhu, Da Chen, "Mechanism Research on the influence of Large Scale Wind power integration on Power System Angle stability," *ELsevier Energy Procedia*, vol. 145, no. 2018, pp. 295-300, 2018.
- [9] Vittal, E.; O'Malley, M.; Keane, " Rotor Angle Stability with High Penetrations of Wind Generation," *Power Syst. IEEE Trans.*, vol. 27, pp. 38-47, 2012.
- [10] Margaris, I.D.; Papathanassiou, S.A.; Hatziaargyriou, N.D.; Hansen, A.D.; Sorensen, P., "Frequency Control in Autonomous Power Systems with High Wind Power Penetration.," *IEEE Trans. Sustain. Energy*, vol. 3, pp. 189-199, 2012.
- [11] Zhang, Z.S.; Sun, Y.Z.; Lin, J.; Li, G.J. , " Coordinated frequency regulation by doubly fed induction generator-based wind power plants.," *Renew. Power Gener. IET*, vol. 6, pp. 38-47, 2012.
- [12] J.B. Ekanayake, L. Holdsworth, X. Wu and N. Jenkins, "Dynamic modeling of doubly fed induction generator wind turbines," *IEEE Trans. on Power Systems*, vol. 18, pp. 803-809, 2003.
- [13] S.M. Muyeen, H.A. Mohd, R. Takahashi, T. Tamura, Y. Tomaki, A.Sakahara and E. Sasano., "Transient stability analysis of wind generator system with the consideration of multi-Mass shaft model,," in *International Conference on Power Electronics and Drives Systems*, 2005.
- [14] Y.Z. Lei, A. Mullane, G. Lightbody, R. Yacamini,, "Modeling of the wind turbine with a doubly fed induction generatorfor grid integration studies," *IEEE Trans. on Energy Conversion*, vol. 21, pp. 257-264, 2006.
- [15] M. EL-Shimy, M.A.L Badr, and O.M.RASSEM, "IMPACT OF LARGE SCALE WIND POWER ON POWER SYSTEM STABILITY," in *IEEE Conference on Energy Systems*, 2008.
- [16] Libao Shi, Shiqiang. Dai, Yixin Ni, Liangzhong Yao, and Masoud Bazargan, "Transient Stability of Power Systems with High Penetration of DFIG Based Wind Farms," *IEEE Power Transactions*, 2009.
- [17] Samuel Adi Kusumo, Tiyono, Lesnanto Multa Putranto, "Transient Stability Study in Grid Integrated Wind Farm," in *International Conference on Technology, Computer and Electrical Engineering*, 2018.
- [18] Md Ayaz Chowdhury, Weixiang Shen, Nasser Hosseinzadez, Hemanshu Roy Pota, "Transient stability of power system integrated with doubly fed induction generator wind farms," *IET Renewable Power Generation*, vol. 9, no. 2, 2015.
- [19] Shiwei Xia , Qian Zhang , S.T. Hussain, Baodi Hong and Weiwei Zou, "Impacts of Integration of Wind Farms on Power System Transient Stability," *MDPI Applied Sciences*, vol. 8, pp. 1-16, 2018.
- [20] Luis Arturo Soriano, Wen Yu, and Jose de Jesus Rubio, "Modeling and Control of Wind Turbine," *Mathematcial Problems in Engineering*, vol. 2013, pp. 1-14, 2013.



INNO  **SPACE**
SJIF Scientific Journal Impact Factor

Impact Factor:
7.122

ISSN INTERNATIONAL
STANDARD
SERIAL
NUMBER
INDIA



International Journal of Advanced Research

in Electrical, Electronics and Instrumentation Engineering

 **9940 572 462**  **6381 907 438**  **ijareeie@gmail.com**



www.ijareeie.com

Scan to save the contact details